Available online at www.sciencedirect.com
ScienceDirect
Trans. Nonferrous Met. Soc. China 24(2014) 2266−2274
Transactions of Nonferrous Metals Society of China
www.tnmsc.cn

Precipitation of metastable phases and its effect on electrical resistivity of Al−0.96Mg_2Si alloy during aging

Li-xin CUI[1], Zhen-xing LIU[2], Xiao-guang ZHAO[1], Jian-guo TANG[2], Ke LIU[1], Xing-xing LIU[2], Chen QIAN[2]

1. Shandong Innovation Alloy Institute, Zouping 256200, China;
2. School of Materials and Engineering, Central South University, Changsha 410083, China

Received 17 October 2013; accepted 22 May 2014

Abstract: The precipitation behavior and its influence on the electrical resistivity of the Al−0.96Mg_2Si alloy during aging were investigated with in-situ resistivity measurement and transmission electron microscopy (TEM). The precipitates of the peak aged alloy include both β'' and β', but the amount ratio of β'' to β' varies with the aging temperature and time increasing. The precipitates during aging at 175 °C are dominated by needle-like β'' phases (including pre-β'' phase), the size of which increases with the time prolonging, but does not increase substantially after further aging. The evolution of electrical conductivity is directly related to such microstructural evolution. However, the hardness of the alloy stays at the peak value for a long term. When the alloy is aged at 195 °C, the ratio of β'' to β' becomes the main factor to influence relative resistivity ($\Delta\rho$) value. The higher the temperature is, the smaller the ratio is, and the faster the $\Delta\rho$ value decreases. Moreover, the hardness peak drops with the decrease of the ratio. With the size and distribution parameters measured from TEM images, a semi-quantitative relationship between precipitates and the electrical resistivity was established.

Key words: Al−Mg−Si alloy; metastable phases; electrical resistivity; aging; precipitate

1 Introduction

6000 series aluminium alloys have been widely used because of their moderate properties for industrial and technological feasibility [1]. The 6101/6101A and 6201 alloys have less alloying elements compared with other Al−Mg−Si alloys. As a result of exponential strengthening rate in hardness and logarithmic increasing rate in conductivity with aging time, the alloys are utilized extensively in power supply [2,3] and electronic applications. The precipitation sequence and mechanisms for strengthening of Al−Mg−Si alloy have been determined as [4−6]: supersaturated solid solution (SSS) → Si/Mg-clusters → co-clusters → GP(I) zones (→ pre-β'' phase) → β'' phase → β' phase → β phase. With more coherency and less strain to the matrix, the pre-β'' phase, which has the same structure with β'' phase, is hard to be distinguished by conventional TEM but HRTEM [7]. Researchers have indicated that the coherent β'' phase, with monoclinic structure and lattice parameters: a=1.516 nm, b=0.405 nm, c=0.674 nm (β=105.3°), is the main strengthening precipitate in Al−Mg−Si alloys [8−11]; the semi-coherent β' phase, with hexagonal structure and lattice parameters: a=0.705 nm, c=1.215 nm [10], has less strengthening effect; the incoherent equilibrium β phase, with the anti-fluorite structure, incoherent to the matrix, has non-hardening effect.

The relationship between electrical resistivity and precipitation of Al−Mg−Si alloys was investigated by several researchers [12,13]. It was found that the formation of clusters increases the resistivity of the as-quenched alloy at the early stage of aging, but finally the resistivity decreases at the peak aging. To understand the effect of the solute concentration and clusters or precipitates on the resistivity, the Matthiessen's law [14,15] was introduced. And both clusters and fine precipitates have strong electron scattering effect [16,17]. The size of crystallographic defects, precipitates, impurities and their distribution in the alloys will influence the resistivity significantly, with the similar magnitude of the mean free path of the electron. RAEISINIA et al [15] found that the effect of the precipitates' size on the resistivity (contribution of their

Foundation item: Project (51105139) supported by the National Natural Science Foundation of China; Project (2010CB731706) supported by the National Basic Research Program of China
Corresponding author: Zhen-xing LIU; Tel: +86-731-88830265; E-mail: jgtang@csu.edu.cn
DOI: 10.1016/S1003-6326(14)63343-4

distribution ρ_{ppt}) must be considered in the model and obtained an equation for AA6111. Nevertheless, the effect of the precipitates' distribution of the Al−Mg−Si alloy during aging is not clear in quantity.

In order to investigate the details of the influence of β'' phases on the resistivity, which most commonly exist in commercial electrical alloys, the effect of the microstructures of 6101A alloy during aging on the resistivity, the precipitates' size and their distribution is investigated in the present study.

2 Experimental

The boronised Al−2.74%B master alloy with chemical composition shown in Table 1, in which the Mg−Si is balanced according to Eq. (1) reported by GUPTA et al [11], was extruded at 450 °C, then solutionized at 505 °C for 2 h, and finally aged at 175 °C, 185 °C and 195 °C after water-quenching to room temperature. In order to avoid the detrimental effect of natural aging, the as-quenched samples were transferred from quenching container to aging furnace within 5 min.

$$\text{Excess Si}=m(\text{Si})-m(\text{Mg})/1.73-m(\text{Fe})/4 \quad (1)$$

Table 1 Composition of experimental alloy (mass fraction, %)

Si	Mg	Fe	Na	Ca	V
0.378	0.613	0.123	0.025	0.012	0.007

Ti	Others		Al	Mg_2Si	Excess Si
	Single	Total			
0.002	<0.01	<0.03	98.8	0.96	−0.007

Vickers hardness measurement after aging was performed using Model HV−10B instrument at 29.4 N load. There were two samples for each heat treatment, and five hardness data were taken for each sample while the average values were used. The non-isothermal in-situ resistivity was measured with heating rate of (10±1) °C/min from 20 °C to 550 °C, and the isothermal in-situ resistivity during aging was measured at the tested temperature fluctuated by ±1 °C in atmosphere by double bridge, after holding for 20 min. The resistivity-tested specimens were cut in dimensions of ~3 mm × 5 mm × 70 mm. The measured electrical resistivity of the Al−0.96Mg_2Si alloy after water-quenching is changed into the relative resistivity ($\Delta\rho$) for convenient comparison by

$$\Delta\rho=\frac{\rho-\rho_0}{\rho_0}\times 100\% \quad (2)$$

where ρ is the specific electrical resistivity of the alloy; ρ_0 is a reference in the measured condition; $\Delta\rho$ is the relative change of the resistivity ρ to ρ_0.

Microstructural characterization of the alloy was carried out on a TECNAIG^2 20 transmission electron microscope (TEM) with operating voltage of 200 kV. The samples were prepared by twin-jet electro polishing after mechanically grinding to a thickness of 80 μm, with a solution of 20% nitric acid and 80% methanol at −25 °C. The size parameters of precipitates were measured by the software Image J from average values of at least 5 images.

3 Results and analysis

3.1 Evolution of electrical resistivity during non-isothermal heating

In Fig. 1, ρ_0 is the resistivity at room temperature, and the $\Delta\rho$ value is the relative increment. As precipitation also has strong effect on the resistivity, the high purity aluminum (99.998%) is used as a reference in Fig. 1. The resistivity variation between the investigated alloy and the high purity aluminum can be ascribed to precipitation [12]. The distinct changes of the slopes of the two lines in Fig. 1 in the temperature range of ~270 °C to ~350 °C could be ascribed to the precipitating result of β'' and β' phases. Figure 2 shows the typical needle-like β'' and rod-like β' precipitates of the alloy, treated at 250 °C and 300 °C, respectively, along the direction ⟨100⟩ with distinct strain contrast [9,11,18−22]. The evolution of the resistivity can be explained by the modified form of Matthiessen' law [15]:

$$\rho=\rho_{\text{pure}}(T)+\sum_i \rho_i C_i+\rho_{\text{ppt}} \quad (3)$$

where $\rho_{\text{pure}}(T)$ is the resistivity of pure metal at temperature T, $\rho_i C_i$ is the resistirity of the ith solute at concentration of C_i, and ρ_{ppt} is the contribution of the

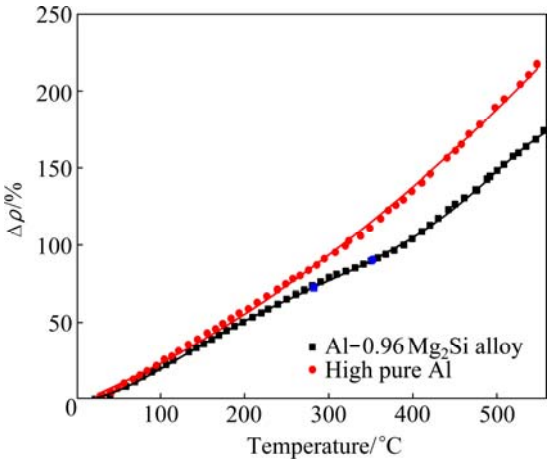

Fig. 1 Non-isothermal in-situ relative electrical resistivity ($\Delta\rho$) curves of Al−0.96Mg_2Si and high purity aluminium at heating rate of (10±1) °C/min

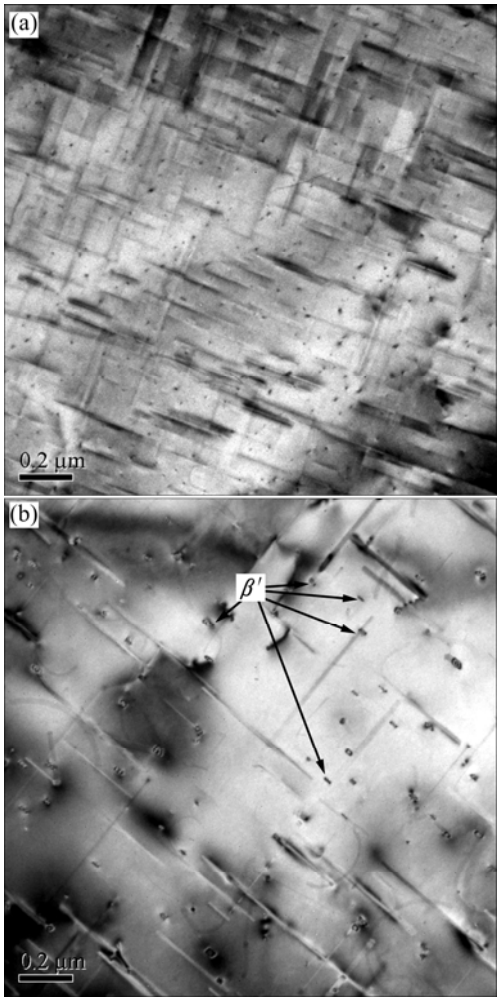

Fig. 2 TEM images of needle-like β'' phase at heating rate of 10 °C/min from room temperature to 250 °C and aged at 250 °C for 5 min after water-quenching (a), and rod-like β' phases at heating rate of 10 °C/min from room temperature to 300 °C and aged at 300 °C for 5 min after water-quenching (b) (Observation direction parallel to [001])

precipitates on resistivity. $\sum_i \rho_i C_i + \rho_{ppt}$ changes with the concentration of solutes and the microstructures of the precipitates. Precipitation of the Al−0.96Mg_2Si alloy in the temperature range of ~250 °C to ~350 °C depletes the solutes in the solid solution, diminishes the effect of the scattering of electrons, and finally leads to the reduction of the $\Delta\rho$ value.

3.2 Evolution of hardness and electrical resisitivity during aging

For the Al−0.96Mg_2Si alloy, the obvious effect of natural aging has been observed at room temperature. DAOUDI et al [23] and GABER et al [18] suggested that the thermally activated phase transformations in Al−Mg−Si alloys are controlled by the diffusion of solute atoms. Therefore, the high temperature favors quick precipitation and fast coarsening of the precipitates. But higher density of the precipitates is required to increase the strength of the alloys while the coarser β'-phase decreases the strength [22]. At the beginning of aging, the rate of strengthening slows (Fig. 3), in which the hardness in the plateau maintains for 5 h at 195 °C, but more than 12 h at 175 °C, and over 6 h for the two-stage aging. The hardness in the plateau is over HV 90 at 175 °C, while near HV 75 at 195 °C, and near HV 85 at 175 °C of two-stage aging. And, the hardness experiences a slight drop after 720 min at 175 °C, and after 540 min at 175 °C of two-stage aging.

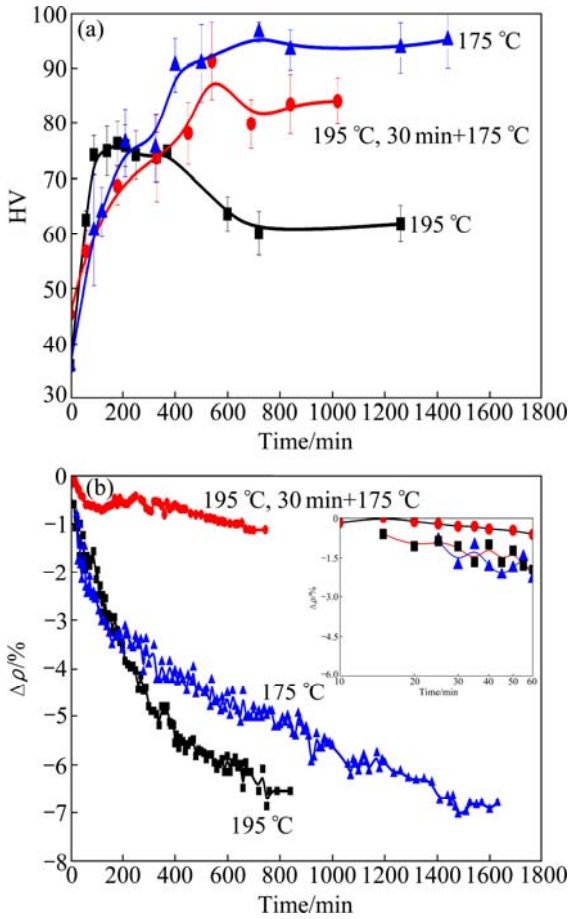

Fig. 3 Vicker hardness (a) and $\Delta\rho$ (b) values of Al−0.96Mg_2Si alloy during aging at different temperatures

The isothermal relative electrical resisitivity obtained by in-situ measurement changes due to the aged microstructure which influences the hardness. In Fig. 3, ρ_0 is the resistivity after aging for 20 min to stabilize the aging temperature. The relative resistivity of the alloy decreases with time, and surrenders at ~60 min and ~150 min when aged at 175 °C. While the hardness curve surrenders were delayed to ~120 min and ~200 min. The delay of hardness evolution means that the resistivity is more senstive than the hardness to the microstructural transformations. At the initial stage of aging, the two-stage aged alloy has the highest relative resistivity, then

at 195 °C and finally at 175 °C. When the aging time exceeds 150 min, the relative resistivity of the one aged at 175 °C exceeds that of the one aged at 195 °C, but is still less than that of the two-stage aged one. The higher the temperture is, the more the clusters are in the early stage of aging, and the preaging at 195 for 30 min forms more clusters and GP zones. The formation of these clusters and GP zones accounts for the evolution of relative resistivity at the initial stage of aging. But the metastable clustes would dissolve and form new precipitates such as pre-β'' and/or β'' with prolonging aging time, and high temperature aging also favors such process. Therefore, precipitates of β'' , β' and β dominate the whole aging process except for the clusters dominated initial stage.

3.3 Evolution of precipitates during aging

The average diameter (d), length (l), area fraction (f_A), and planar number densitiy (N_p) of the precipitates in the alloy during aging at 175 °C and two-stage aging measuremed from TEM images are shown in Table 2. The pre-β'' phase can exist at 175 °C before 720 min (Fig. 3), refered to the work of MARIOARA et al about pre-β'' [7]. When the alloy is aged at 175 °C, from 210 min on, the average size of the precipitates changes slightly, but the density changes violently. POGATSCHER et al [24] found that dozens of days' or a short-term natural aging brought vacancy-rich co-clusters (vacancy-prison) out, which were temporarily stabilized at high temperature and too small to act as nucleation sites directly [25], but dissolved at a higher aging temperature to release vacancies for nucleation of precipitates. In the present study, due to about 5 min delay after water-quenching, a short-term natural aging can prison a certain amount of vacancies. It is likely to be a reason to the linear increase of the $\Delta\rho$ value, and probably related to the decrease of dH_V/dt in aging close to 320 min because of the dissolution of vacancy-prisons. The released vacancies may help to increase the density of the precipitates in the following aging, but the small size of the new-nucleated precipitates retains the mean size steady. A certain amount of newly nucleated short needle-like β'' (pre-β'') phases between the growing and the stabilized β'' precipitates and the plentiful transformation from GP zones (or clusters) to β'' (or pre-β'') phases increase the area fraction (f_A) and the planar number densitiy (N_p), when lots of short β'' (or pre-β'') phases occur as the time prelongs (Fig. 4). After being preaged at 195 °C for 30 min, the precipitates are the same as that aged at 175 °C for 60 min, lots of clusters, few GP zones and pre-β'' phases are included (Fig. 5(a)). The density increases as the time prolongs, but the size of β'' phases retains at (3±0.1) nm approximately.

When the alloy is aged at higher temperature (195 °C), the type of the precipitates changes, and the quantity and size are different. Figure 5(c) (aged at 195 °C for 60 min) shows that not only needle-like β'' phase but also rod-like β' phase appears. The precipitates in Fig. 5(c) are obviously larger and longer than those in Fig. 4 and Figs. 5(a), (b), up to 100 nm for needle-like β'' phases and around 60 nm for rod-like β' phases. Before the hardness decreases sharply, the amount ratio (R) of precipitates β'' and β' at 195 °C decreases with the temperature increasing and time prolonging ($R_{175\ °C}=+\infty$, $R_{195\ °C,\ 60\ min}=2-3$, $R_{195\ °C,\ 210\ min}=0.8-1.3$). The activation energies of β'' phase and β' phase are 76 kJ/mol and 117 kJ/mol [18], respectively, calculated by Kissingers' method, which means that β' phase is more difficult to nucleate at low temperature. Therefore, the ratio of β''/β' varies depending on the temperature signifiantly. The high quantity of the precipitates ($N_{195\ °C}$) determines the high rate of strengthening dH_V/dt, the high ratio of precipitates β''/β' ($R_{175\ °C}$) determines the high peak hardness. In the hardness plateau at 195 °C, the low ratio of β''/β' declines for the rapid transformation from β'' phase to β' phase, which consumes the coherency to the Al matrix steeply (Fig. 6). Meanwhile, β' phase grows more easily than β'' phase [23], thus the hardness plateau at 195 °C is shorter. When extending the aging time, the density and the size of rod-like β' increase, as shown in Fig. 5(d) (195 °C, 210 min).

Table 2 Average diameter (d), length(l), area fraction (f_A), planar number densitiy (N_p) of precipitates in alloy during aging

Aging	d/nm		l/nm		$N_p/10^3\mu m^{-2}$	f_A/%
	Mean	Range	Mean	Range		
175 °C, 60 min	1.9±0.43	1.2−2.7	1.9±0.43	1.2−2.7	0.45±0.03	0.21±0.05
175 °C, 210 min	3.0±0.45	1.2−3.8	15±7	5−60	1.48±0.23	1.7±0.28
175 °C, 320 min	3.1±0.55	1.2−4.5	27±20	5−150	1.61±0.06	2.9±0.55
175 °C, 720 min	3.1±0.58	1.2−4.5	21±15	5−180	3.17±0.16	6.5±1.1
195 °C, 30 min	2.0±0.56	1.2−3.2	2.0±0.56	1.2−3.2	0.33±0.05	0.25±0.05
(195 °C, 30 min) + (175 °C, 540 min)	2.9±0.37	1.9−4.0	10±2.5	5−40	3.79±0.68	4.92±0.69

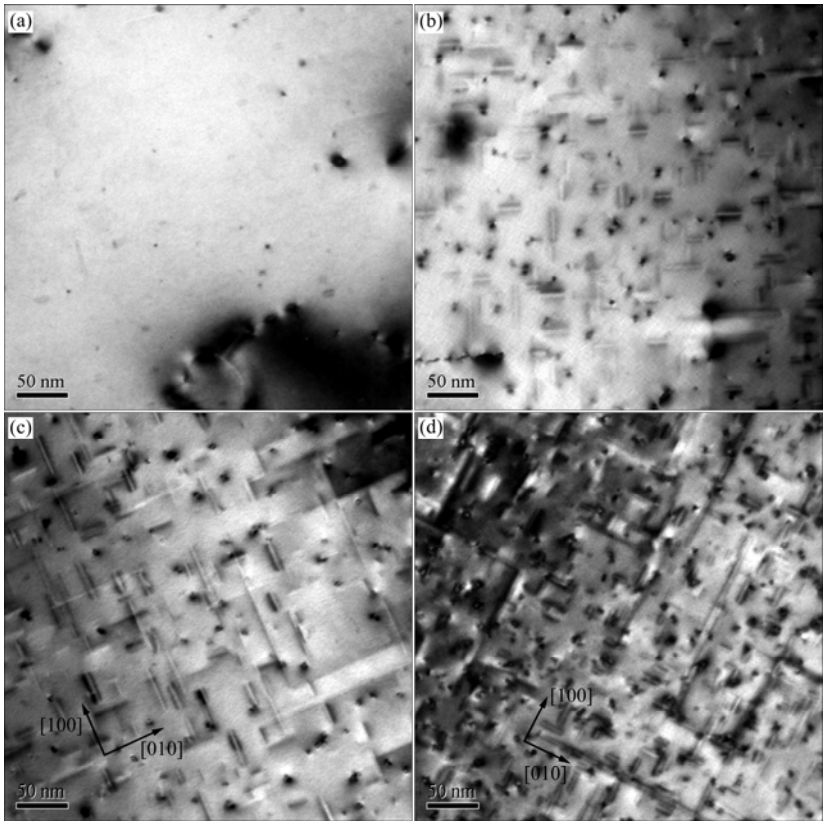

Fig. 4 Evolution of precipitates during aging at 175 °C (Observation direction parallel to [001]): (a) 60 min; (b) 210 min; (c) 320 min; (d) 720 min

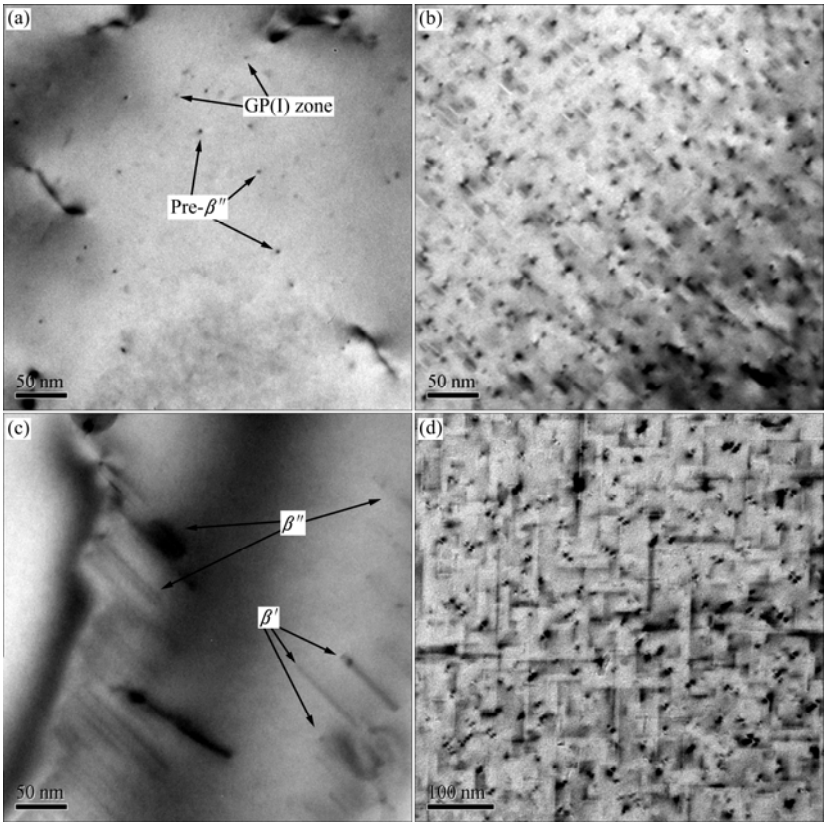

Fig. 5 Influence of aging on precipitates (Obsrvation direction parallels to [001]): (a) 195 °C, 30 min; (b) (195 °C, 30 min) + (175 °C, 540 min); (c) 195 °C, 60 min; (d) 195 °C, 210 min

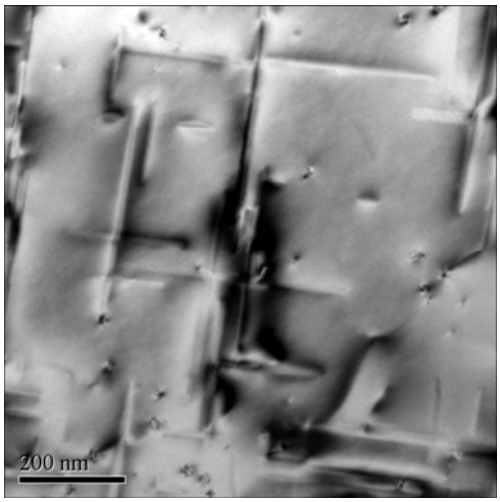

Fig. 6 Precipitates of alloy overaged at 195 °C for 720 min (Observation direction parallel to [001])

4 Discussion

YUAN et al [26] investigated the effects of multiple precipitates on the electrical conductivity of Al−Mg−Si alloys aged at 200 °C and 300 °C, and found that this effect was dominated by those closely spaced fine precipitates which result in severe electronic scattering. The main influential precipitates could firstly be β'' phase and then β' phase, but the details are very complicated. Figures 4 and 5 show that, only the β'' phase (taking pre-β'' phase as β'' phase) appears in a long-term aging at 175 °C and two-stage aging, so the area fraction (f_A) and the size of the prepitates are the main factors affecting $\Delta\rho$.

Substituting Eq. (3) for ρ into Eq. (2), it changes to

$$\Delta\rho = \rho_0^{-1} \cdot \left[-\left(\sum_i \rho_i \Delta C_i \right) + \rho_{\text{ppt}} \right] \tag{4}$$

where ΔC_i is the concentration variation of the ith solute atom, $\sum_i \rho_i \Delta C_i$ is the variation of the electrical resistivity resulting from the descending of solutes in solid solution. Refering to the work of RAEISINIA et al [15], the concentration variations of Mg and Si due to the precipitate $\beta''$are

$$\Delta C_{\text{Mg}}=0.42 f_{\text{A}};\ \Delta C_{\text{Si}}=0.51 f_{\text{A}} \tag{5}$$

and ρ_{ppt} can be expressed as [16]

$$\rho_{\text{ppt}} = \frac{12}{\lambda^{1/2}} \tag{6}$$

where λ is the spacing between the precipitates. The Mg and Si solutes in solid solution increase the resistivity of the Al matrix by 5.5×10^{-9} Ω·m per 1% (mole fraction) Mg and 6.9×10^{-9} Ω·m per 1% (mole fraction) Si at room temperature, respectively. The mean diameter and length of the precipitates can be measured by TEM, so as the area fraction and the planar number density, though a considerable deviation with the true parameters has been included. λ can be estimated as [27]

$$\lambda = \left(\frac{2\pi \times 100}{f_{\text{A}}} \right)^{1/2} \cdot \frac{d}{2} \tag{7}$$

Semi-quantitative calculation of the spacing (λ), ρ_{ppt} and the ratio of $\rho_{\text{ppt}} / \sum_i \rho_i \Delta C_i$ indicates the contribution of the size and the distribution of the precipitates (Table 3). The precipitation of β'' decreases the relative conductivity by at least 8% for single aging, and by 10% for two-stage aging because of higher density precipitates. At the early stage of aging the clusters act as scattering sites of the free electrons, since the size of equiaxed particles or solute-vacancies is in the similar magnitude of the mean free path of the electron. Meanwhile, a few precipitates form so that the ratio $\rho_{\text{ppt}} / \sum_i \rho_i \Delta C_i$ is larger than 1 except for clusters. In fact, the $\Delta\rho$ value after aging at (175 °C, 60 min) doesn't increase, and the $\Delta\rho$ in the early stage at 195 °C in two-stage aging retains as well, as in the insert graph in Fig. 3. It may be attributed to the inhomogeneous local composition of the alloy because some clusters have transformed to GP-zones (or pre-β'' precipitates). The contribution of the precipitates on resistivity increases with the aging time but that of solute atoms on resistivity caused by precipitation decreases more. The relative electrical resistivity $\Delta\rho$ decreases finally. Equation (4) is depicted with λ and f_A as

$$\Delta\rho = \rho_0^{-1}(-5.9 f_{\text{A}} + 3.4 f_{\text{A}}^{1/4} \cdot d^{-1/2}) \tag{8}$$

which is the complete expression to describe the $\Delta\rho$ (characterization of the increment of the conductivity) in 6101 or 6201 balanced alloy when aging at 175 °C, with

Table 3 Spacing (λ), ρ_{ppt} and $\rho_{\text{ppt}} / \sum_i \rho_i \Delta C_i$ of precipitates in alloy during aging

Aging	λ/nm	$\rho_{\text{ppt}}/(10^{-9}\Omega\cdot\text{m})$	$\rho_{\text{ppt}} / \sum_i \rho_i \Delta C_i$
175 °C, 60 min	52±4.8	1.67±0.08	1.34
175 °C, 210 min	29±2.4	2.24±0.1	0.22
175 °C, 320 min	23±1.5	2.52±0.08	0.15
175 °C, 720 min	15±1.7	3.08±0.17	0.08
195 °C, 30 min	50±8.6	1.72±0.16	1.15
(195 °C, 30 min) + (175 °C, 540 min)	16±1.4	2.96±0.12	0.10

one kind of precipitate β'' phases. The contribution of precipitates, which accounts for 10%−20% of the resistivity variation in dozens of nanometers of spacing, can be estimated semi-quantitatively by

$$\rho_{\text{ppt}} / \sum_i \rho_i \Delta C_i = 0.58 f_{\text{A}}^{-3/4} \cdot d^{1/2} \quad (9)$$

Figure 7 reveals that a large number of nuclei form when the alloy is aged at 175 °C in the first 250 min, and then they grow fast. The constant n for JMA-formula is temperature dependent and calculated as: n=1.34 for 175 °C, and n=1.19 for 175 °C in two-stage aging. The constant n=1.34 means that nucleating dominates the early stage of the phase transformation, and n=1.19 means that the growth dominates the phase transformation. The mean diameter (d) and the planar number density (N_{p}) increase linearly. However, after 300 min the trend goes to the contrary: slow growth of precipitates and continuous nucleation which is slower than that in the beginning as the concentration decreases. The newly nucleated β'' between the previously formed β'' precipitates makes the average size and spacing between the precipitates decrease. Newly nucleated nuclei slow down the increase of the precipitates mean size, but a long-term heterogeneous nucleation increases the planar number density N_{p} fast at first and then slows down. In Fig. 7, the planar number density N_{p} changes consistently with the ascending tendency of the $\Delta\rho$ value. When prolonging the aging time over 200 min, the distribution of the precipitates plays a dominant role in the increasing of the $\Delta\rho$. The size of the new nuclei and the decreased spacing between the precipitates are of the same magnitude as the mean free path of the electron, with severe electronic scattering. The $\Delta\rho$ value decreases with a slow rate after 320 min as a result of new nucleation. Thus, this aluminum alloy should be aged at least 320 min to obtain a stable size of precipitates for conducting application in aging at 175 °C.

A considerable deviation has been included in the precipitates' parameters measured from TEM images, but the details are clear in quantity, so the calculated results are semi-quantitative. If the accurate quantitative calculation is applied, the small-angle X-ray scattering (SAXS) or small-angle neutron scattering (SANS) is necessary for the measurement of the precipitates' parameters. To produce an aluminum alloy with high conductivity (>60% IACS) and moderate strength ($\sigma_{0.2}$≥ 200 MPa), firstly the strengthening β''-phase should be

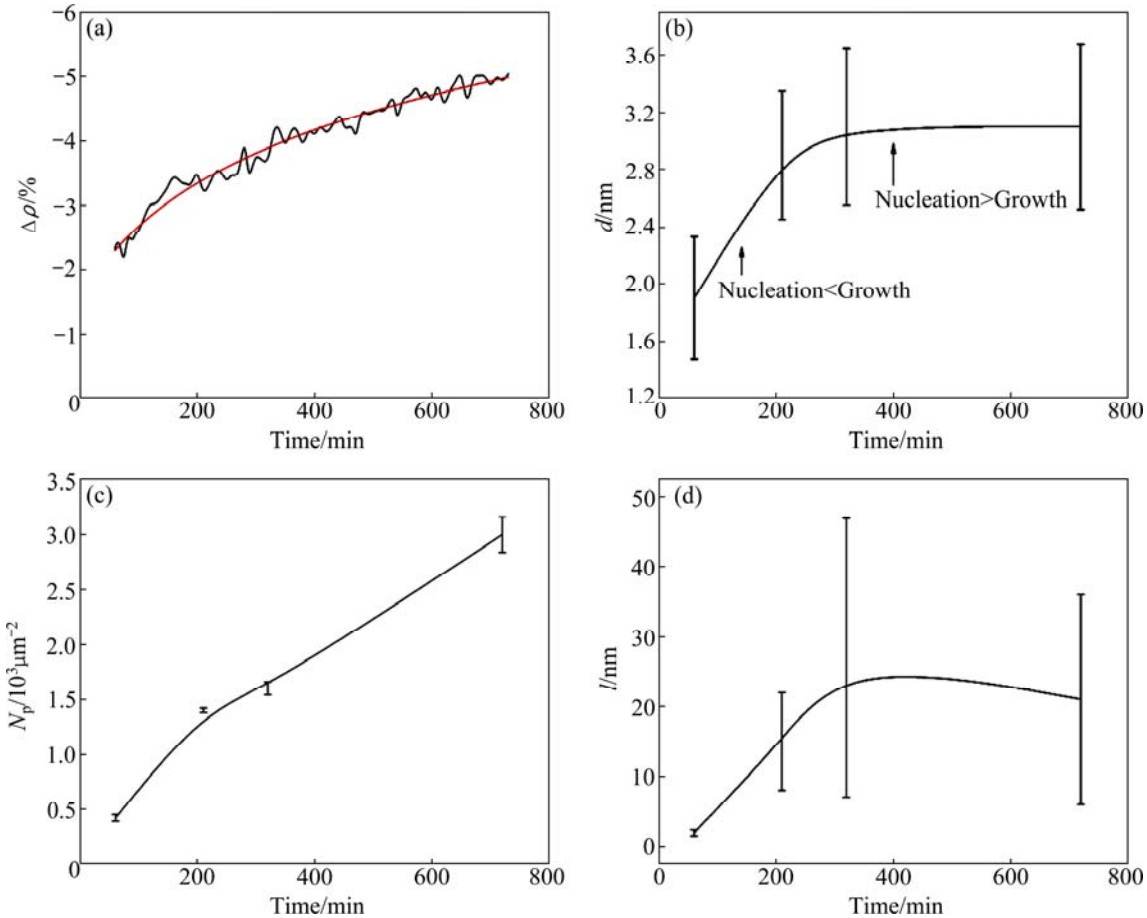

Fig. 7 Evolution of precipitates' parameters during aging at 175 °C: (a) $\Delta\rho$ values (smooth full line gives increasing tendency); (b) Mean diameter, (c) Planar number density; (d) Mean length of precipitates

introduced to ensure the strength when reducing the adverse effect of the solute alloying element (Mg, Si) on the conductivity, and then the spacing between the precipitates λ should be controlled as large as possible to reduce ρ_{ppt} by a suitable aging treatment.

5 Conclusions

1) The precipitates of the peak aged alloy include: only needle-like β'' phase (pre-β'' phase included) at 175 °C both in single and two-stage aging, and both β'' phase and rod-like β' phase at 195 °C. The amount ratio of β'' to β' varies with the temperature and the time. The higher the temperature is and the longer the aging time is, the smaller the ratio is.

2) The influence of precipitates density ρ_{ppt} and solute concentration ΔC_i on the electrical resistivity of the investigated alloy can be estimated as

$$\rho_{ppt} / \sum_i \rho_i \Delta C_i = 0.58 f_A^{-3/4} \cdot d^{1/2}$$

For the single aging at 175 °C, $\rho_{ppt} / \sum_i \rho_i \Delta C_i$ decreases from 0.22 to 0.08.

3) During aging at 175 °C solely, the β'' phases are nucleating for a long time but the growth of nuclei maintains after 320 min, by which the distribution contribution of precipitates (ρ_{ppt}) has been increased.

References

[1] ZENG F L, WEI Z L, LI J F, LI C X, TAN X, ZHANG Z, ZHENG Z Q. Corrosion mechanism associated with Mg_2Si and Si particles in Al–Mg–Si alloys [J]. Transactions of Nonferrous Metals Society of China, 2011, 21(12): 2559−2567.

[2] KARABAY S. Modification of AA-6201 alloy for manufacturing of high conductivity and extra high conductivity wires with property of high tensile stress after artificial aging heat treatment for all-aluminium alloy conductors [J]. Materials & Design, 2006, 27(10): 821−832.

[3] KARABAY S. Influence of AlB_2 compound on elimination of incoherent precipitation in artificial aging of wires drawn from redraw rod extruded from billets cast of alloy AA-6101 by vertical direct chill casting [J]. Materials & Design, 2008, 29(7): 1364−1375.

[4] BANHART J, CHANG C S T, LIANG Z Q, WANDERKA N, LAY M D H, HILL A J. Natural aging in Al−Mg−Si alloys−A process of unexpected complexity [J]. Advanced Engineering Materials, 2010, 12(7): 559−571.

[5] SHENG X F, YANG W C, XIA C D, GONG J, WANG M P, LI Z, ZHANG Q. Effects of T6 and T6I6 ageing treatments on microstructure and properties of 6005A aluminum alloy [J]. The Chinese Journal of Nonferrous Matals, 2012, 22(5): 1276−1282. (in Chinese)

[6] LI H, WANG X L, SHI Z X, WANG Z X, ZHENG Z Q. Precipitation behaviors of Al−Mg−Si−(Cu) aluminum alloys during continuous heating [J]. The Chinese Journal of Nonferrous Matals, 2011, 21(9): 2028−2034. (in Chinese)

[7] MARIOARA C D, ANDERSEN S J, JANSEN J, ZANDBERGEN H W. The influence of temperature and storage time at RT on nucleation of the β'' phase in a 6082 Al–Mg–Si alloy [J]. Acta Materialia, 2003, 51(3): 789−796.

[8] ANDERSEN S J, ZANDBERGEN H W, JANSEN J, TRÆHOLT C, TUNDAL U, REISO O. The crystal structure of the β'' phase in Al–Mg–Si alloys [J]. Acta Materialia, 1998, 46(9): 3283−3298.

[9] EDWARDS G A, STILLER K, DUNLOP G L, COUPER M J. The precipitation sequence in Al–Mg–Si alloys [J]. Acta Materialia, 1998, 46(11): 3893−3904.

[10] VISSERS R, van HUIS M A, JANSEN J, ZANDBERGEN H W, MARIOARA C D, ANDERSEN S J. The crystal structure of the β' phase in Al–Mg–Si alloys [J]. Acta Materialia, 2007, 55(11): 3815−3823.

[11] GUPTA A K, LLOYD D J, COURT S A. Precipitation hardening in Al–Mg–Si alloys with and without excess Si [J]. Materials Science and Engineering A, 2001, 316(1–2): 11−17.

[12] GAFFAR M A, GABER A, MOSTAFA M S, ABO ZEID E F. The effect of Cu addition on the thermoelectric power and electrical resistivity of Al–Mg–Si balanced alloy: A correlation study [J]. Materials Science and Engineering A, 2007, 465(1−2): 274−282.

[13] SEYEDREZAI H, GREBENNIKOV D, MASCHER P, ZUROB H S. Study of the early stages of clustering in Al–Mg–Si alloys using the electrical resistivity measurements [J]. Materials Science and Engineering A, 2009, 525(1−2): 186−191.

[14] MATSUMOTO K, KOMATSU S Y, IKEDA M, VERLINDEN B, RATCHEV P. Quantification of volume fraction of precipitates in an aged Al−1.0 mass%Mg_2Si alloy [J]. Materials Transactions, 2000, 41(10): 1275−1281.

[15] RAEISINIA B, POOLE W J, LLOYD D J. Examination of precipitation in the aluminum alloy AA6111 using electrical resistivity measurements [J]. Materials Science and Engineering A, 2006, 420(1−2): 245−249.

[16] ROSSITER P L, WELLS P. The dependence of electrical resistivity on short-range order [J]. Journal of Physics, 1971, 4: 354−363.

[17] HILLEL A J, EDWARDS J T, WILKES P. Theory of the resistivity and Hall effect in alloys during Guinier-Preston zone formation [J]. Philosophical Magazine, 1975, 32(1): 189−209.

[18] GABER A, GAFFAR M A, MOSTAFA M S, ZEID E F A. Precipitation kinetics of Al–1.12Mg_2Si–0.35Si and Al–1.07Mg_2Si–0.33Cu alloys [J]. Journal of Alloys and Compounds, 2007, 429(1−2): 167−175.

[19] PANIGRAHI S K, JAYAGANTHAN R, PANCHOLI V, GUPTA M. A DSC study on the precipitation kinetics of cryorolled Al 6063 alloy [J]. Materials Chemistry and Physics, 2010, 122(1): 188−193.

[20] YASSAR R S, FIELD D P, WEILAND H. The effect of predeformation on the β'' and β' precipitates and the role of Q′ phase in an Al–Mg–Si alloy; AA6022 [J]. Scripta Materialia, 2005, 53(3): 299−303.

[21] WANG S, MATSUDA K, KAWABATA T, YAMAZAKI T, IKENO S. Variation of age-hardening behavior of TM-addition Al–Mg–Si alloys [J]. Journal of Alloys and Compounds, 2011, 509(41): 9876−9883.

[22] MOSTAFA M, BAHMAN M. Influence of sequence of cold working and aging treatment on mechanical behaviour of 6061 alumimun alloy [J]. Transactions of Nonferrous Metals Society of China, 2012, 22(9): 2072−2079.

[23] DAOUDI M I, TRIKI A, REDJAIMIA A. DSC study of the kinetic parameters of the metastable phases formation during non-isothermal annealing of an Al–Si–Mg alloy [J]. Journal of Thermal Analysis and Calorimetry, 2010, 104(2): 627−633.

[24] POGATSCHER S, ANTREKOWITSCH H, LEITNER H, EBNER T, UGGOWITZER P J. Mechanisms controlling the artificial aging of Al–Mg–Si alloys [J]. Acta Materialia, 2011, 59(9): 3352−3363.

[25] MURAYAMA M, HONO K, SAGA M, KIKUCHI M. Atom probe studies on the early stages of precipitation in Al–Mg–Si alloys [J].

Materials Science and Engineering A, 1998, 250(1): 127−132.

[26] YUAN S, PU X, ZHANG G, LIU G, WANG R, SUN J, CHEN K H. Effects of multiple precipitates on electrical conductivity of aged AI−Mg−Si alloys [J]. The Chinese Journal of Nonferrous Metals, 2010, 20(11): 2070−2074. (in Chinese)

[27] NIE J F, MUDDLE B C, POLMEAR I J. The effect of precipitate shape and orientation on dispersion strengthening in high strength aluminium alloys [J]. Materials Science Forum, 1996, 217−222: 1257−1262.

Al−0.96Mg_2Si 合金时效过程亚稳相析出行为及其对合金电阻率的影响

崔立新[1]，刘振兴[2]，赵晓光[1]，唐建国[2]，刘 科[1]，刘星兴[2]，钱 晨[2]

1. 山东创新合金研究院，邹平 256200；
2. 中南大学 材料科学与工程学院，长沙 410083

摘 要：采用原位电阻率测试和透射电镜观察研究 Al−0.96Mg_2Si 合金的析出行为及其对电阻率的影响。发现峰值时效的析出相包括 β''和 β'，而他们的比例随着时效温度和时间的改变而变化。合金在 175 °C 峰值时效内的析出相主要是针状 β''相(也包括 pre-β'')。这些析出相会随着时效时间的延长而长大，但是进一步延长时效时间至超出峰值时效时间后，析出相的尺寸变化并不显著。合金电导率的变化规律与之类似。合金硬度峰值时效后，继续时效很长一段时间硬度变化都不显著。由于温度是影响 β''/β'比的主要因素，因此时效温度也是影响电阻率的主要因素。时效温度越高 β''/β'的比值越小，$\Delta\rho$ 下降的速度就越快。硬度也随着该比值的减小而降低。通过对透射电镜照片分析获得析出相的分布参数，建立了析出相与电阻率之间的半定量关系式。

关键词：Al−Mg−Si 合金；亚稳相；电阻率；时效；析出相

(Edited by Sai-qian YUAN)